Time and Frequency Synchronization for OTFS

Mohsen Bayat, Arman Farhang

Abstract—In this letter, we propose timing offset (TO) and carrier frequency offset (CFO) estimators for orthogonal time frequency space modulation (OTFS). The proposed estimators do not require any additional training overheads as they deploy the same pilot signal that is used for channel estimation. Hence, no additional training overhead is required for synchronization, thanks to the periodic properties of the pilot signal in the delay-time domain. Our proposed TO estimator finds the start of each OTFS block by searching for a periodic sequence in delay and time dimensions. The CFO is then estimated by finding the mean of the angles of a two-dimensional correlation function at the best timing instant. As a novel aspect of these estimators, the multipath diversity of the channel is exploited to achieve a high estimation accuracy. Finally, we show the efficacy of our proposed synchronization techniques through extensive simulations.

Index Terms—OTFS, synchronization, timing offset estimation, carrier frequency offset estimation.

I. INTRODUCTION

Due to its attractive properties, orthogonal time frequency space modulation (OTFS), [1], has become a strong candidate waveform for the sixth generation wireless networks (6G). These properties include resilience to the time-varying channel effects, backward compatibility with previous generation wireless systems and joint radar and communication capabilities, [2]. Synchronization is a challenge in the design of any practical communication system, [3], specially when the channel is time-varying, [4]. Due to their close relationship, OTFS inherits sensitivity to synchronization errors from orthogonal frequency division multiplexing (OFDM). While there exists a large body of work on the synchronization aspects of OFDM, [5]–[8], OTFS literature on this topic is very limited [9]–[11]. In particular, there is no work on joint timing offset (TO) and carrier frequency offset (CFO) estimation for OTFS.

As the initial work, the authors in [9] designed a random access preamble and developed a TO estimation method for the uplink of OTFS. In this method, the TO estimates need to be fed back to the users as the timing reference for the next uplink transmission. However, these TO reports may become outdated. Thus, the authors in [10], proposed a preamble-based TO and cell identity estimation method in downlink. In this method, a linear frequency modulated (LFM) signal is utilized as a preamble. Both solutions in [9] and [10] are limited to time synchronization and the only work on the frequency synchronization of OTFS can be found in [11]. In this work, the CFO effect is considered as a part of the channel and a joint CFO and channel estimation method using an isolated pilot in the delay-Doppler domain is proposed. The drawback of this technique is that CFO cannot be separated from the channel

Mohsen Bayat and Arman Farhang are with the Department of Electronic and Electrical Engineering, Trinity College Dublin, Dublin 2, Ireland (Email: {bayatm,arman.farhang}@tcd.ie).

estimate. Consequently, the users cannot pre-compensate the CFO before the uplink transmission, [8]. Based on the above, the existing synchronization techniques for OTFS are limited to only TO or CFO estimation while they may require the extra preamble overhead.

Hence, in this letter, we propose TO and CFO estimation techniques for OTFS. Our proposed techniques do not require any additional training overhead as the same pilot that is often utilized for channel estimation in OTFS literature, [12], is also deployed for synchronization. Additionally, for a further reduced overhead, similar to [13], we only use one cyclic prefix (CP) at the beginning of each OTFS block instead of using multiple CPs within each block. The isolated pilot in the delay-Doppler domain that is utilized for channel estimation has periodic properties in the delay-time domain. Being inspired by OFDM literature on synchronization, [5]–[8], we exploit the periodic structure of the pilot signal and develop TO and CFO estimation techniques for OTFS.

The delay-time domain pilot signal has a periodic structure on a given delay bin, i.e., a row on the delay-time grid where the pilot is located. Hence, the start of each OTFS block can be found by searching for this periodic pilot signal on the delay-time grid. To this end, in our proposed TO estimation technique, we form a two dimensional (2D) correlation function to find the TO in delay and time dimensions. The proposed TO estimation technique is attractive to completely asynchronous users as it does not have any acquisition range limitations. Finally, we obtain the CFO by finding the angle of the 2D correlation function at the estimated timing instant. As a novel contribution of this letter, we exploit the multipath diversity of the channel that significantly improves the accuracy of both TO and CFO estimates. To corroborate our claims, we analyze the performance of our proposed TO and CFO estimation techniques through simulations. In our simulations, we study the mean and variance of the TO estimation error and the mean square error (MSE) of the CFO estimates. We also analyze the bit error rate (BER) performance of our proposed synchronization techniques. In this analysis, we show that our proposed TO and CFO estimation techniques lead to the same performance as a fully synchronous system even when the channel is highly time-varying.

II. OTFS PRINCIPLES

OTFS signal at baseband is generated by translating the delay-Doppler domain data symbols to the delay-time domain. This process can be implemented by taking inverse discrete Fourier transform (IDFT) across the Doppler dimension at different delay bins, [14], [15], i.e., the rows on the delay-Doppler grid, see Fig. 1. Considering M delay and N Doppler bins, and the corresponding delay-Doppler domain quadrature amplitude modulated (QAM) data symbols, $D[m,n]$ for $m = 0,\ldots,M-1$ and $n = 0,\ldots,N-1$, the signal samples on the delay-time grid can be obtained as $X[m,l] =$
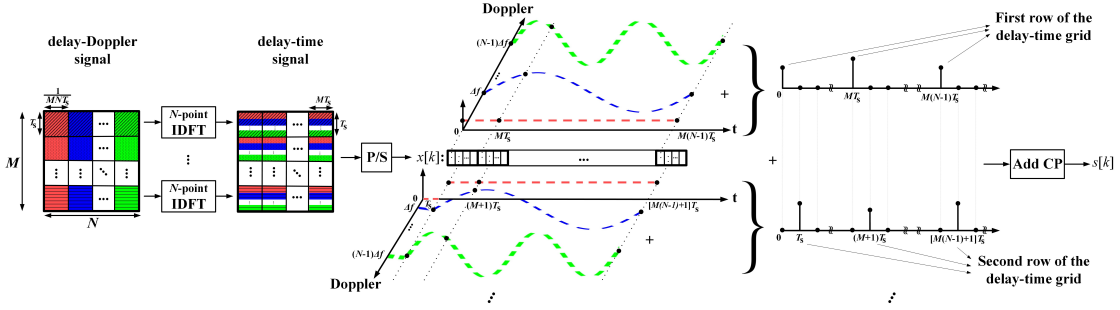
Fig. 1. OTFS signal as a combination of interleaved OFDM signals.

$\frac{1}{\sqrt{N}} \sum_{n=0}^{N-1} D[m,n] e^{\frac{j2\pi ln}{N}}$ where $l = 0, \ldots, N-1$ is the time and m is the delay index. To form the OTFS transmit signal, these samples need to be converted to a serial stream. This is done by concatenating the samples on the columns of the delay-time grid through a parallel-to-serial converter block, i.e., P/S in Fig. 1. Thus, the resulting signal, $x[k]$, takes the values $X[m,l]$ for $k = Ml + m$. From Fig. 1, the OTFS signal before appending the CP can be interpreted as the combination of M up-sampled and delayed OFDM signals, each with N Doppler domain subcarriers. Finally, a CP with the length L_{CP} is appended at the beginning of each OTFS block with MN samples to form the transmit signal $s[k]$. $L_{\mathrm{CP}} \geq L-1$ is chosen to guarantee inter-block interference-free communication where L is the channel length.

The received signal in presence of TO and CFO after transmission over the linear time-varying (LTV) channel can be expressed as

$$r[k] = e^{\frac{j2\pi \varepsilon k}{MN}} \sum_{i=0}^{B-1} \sum_{\ell=0}^{L-1} h[\ell,k] s[k-\ell-\theta-iN_{\mathrm{T}}] + \eta[k], \quad (1)$$

where $\eta[k] \sim \mathcal{CN}(0, \sigma_\eta^2)$ is the complex additive white Gaussian noise (AWGN) with the variance σ_η^2, $N_{\mathrm{T}} = MN + L_{\mathrm{CP}}$ is the OTFS block length, and B is the number of OTFS blocks in each data frame. The variables θ and ε are the normalized TO and CFO values to the delay and Doppler spacings $\Delta\tau = T_{\mathrm{s}}$ and $\Delta\nu = \frac{1}{MNT_{\mathrm{s}}}$, respectively, for a given sampling period T_{s}. $h[\ell,k] = \sum_{i=0}^{\Gamma-1} \alpha_i e^{j2\pi \frac{\kappa_{\max}}{MN}(k-\ell)\cos\psi_i} \delta[\ell-\ell_i]$ is the channel response at the delay-tap ℓ and sample k where Γ, $\kappa_{\max}$, ψ_i, α_i, and ℓ_i are the total number of paths, maximum Doppler shift normalized to the Doppler spacing, the arrival angle, gains and delays corresponding to a given path i, respectively.

III. PROPOSED TO ESTIMATION TECHNIQUE

In this section, we propose a TO estimation technique for OTFS that exploits the periodic properties of the commonly deployed pilot for channel estimation, [12]. Thus, no additional signaling overhead is required for synchronization. Furthermore, our proposed technique does not have any estimation range limitations. Based on the 2D structure of the OTFS block in delay-time domain, we decompose the TO as $\theta = \theta_{\mathrm{d}} + M\theta_{\mathrm{t}}$ where θ_{d} and θ_{t} represent the TO in delay and time, respectively. Then, in the following, we develop a two-stage technique to estimate these offsets.

A. TO estimation in delay dimension

According to the explanations in Section II and Fig. 1, the rows of the delay-time grid are composed of OFDM signals,

each with N Doppler domain subcarriers. On this basis, one may think of adapting OFDM synchronization techniques to OTFS. In pilot patterns (a) and (b), shown in Fig. 2, an impulsive pilot at the delay-Doppler bin $(m_{\mathrm{p}}, n_{\mathrm{p}})$ with the power ρ_{p} is surrounded by zero guard symbols. These pilot patterns are the same as the ones that are used for channel estimation in OTFS literature, [12]. The guard symbols of $2L-1$ and $4(\kappa_{\max} + \hat\kappa) + 1$ along the delay and Doppler dimensions, respectively, are required to avoid interference between the pilot and data symbols caused by the channel, where $\hat\kappa$ is a design parameter, [12]. While our proposed synchronization techniques in this paper work with both pilot patterns, in the following, we consider the pilot pattern (a) for the ease of explanations.

Taking the isolated pilot from delay-Doppler to delay-time domain leads to a constant amplitude sequence on the row m_{p} of the delay-time grid with the linear phase $e^{\frac{j2\pi n_{\mathrm{p}} l}{N}}$ for $l = 0, \ldots, N-1$, i.e., $\sqrt{\rho_{\mathrm{p}}/N}[1, e^{\frac{j2\pi n_{\mathrm{p}}}{N}}, \ldots, e^{\frac{j2\pi n_{\mathrm{p}}(N-1)}{N}}]$. This sequence can be split into two halves with the same amplitude and a constant phase difference of πn_{p}. Thus, the Schmidl and Cox (S&C) method, [5], can be adapted to OTFS. The main assumption of the S&C method is that the two halves of pilot signal remain identical at the channel output. However, this assumption does not hold in LTV channels, as the channel deteriorates the similarity of the two pilot halves. To tackle this issue, the identical parts of the pilot can be brought closer to one another where the time-selective channel only slightly affects the similarity of the adjacent parts. This is inline with the idea of increasing the number of the repetitive parts of the pilot that was proposed to address the limitations of the S&C method in OFDM, [6]. The extreme case for this is when all the pilot samples are the same. Since our pilot has a constant amplitude and a constant phase difference of $2\pi n_{\mathrm{p}}/N$ between the adjacent samples, this extreme case applies to it. Hence, we have the opportunity to develop a TO estimation technique robust to the time variations of the channel for OTFS.

To estimate the TO, we need to search for the pilot sequence on a row of the delay-time grid. Thus, we convert the received signal from serial to parallel, with blocks of M samples in each parallel stream that represent the samples on the columns of the grid. Consequently, we rearrange the received signal as $r[m,l] = r[Ml + m]$ with the delay and time indices m and l, respectively. For a given row m on the delay-time grid, we consider a sliding window with length N that searches for the pilot sequence with N identical samples. This process can be
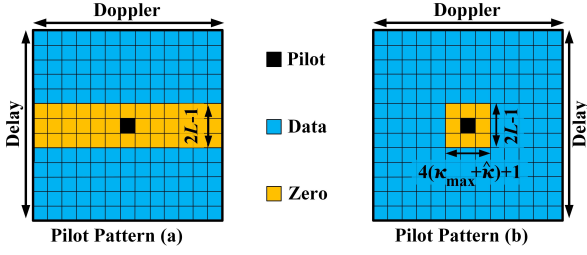
Fig. 2. Pilot patterns in the delay-Doppler domain [12].

implemented by forming the correlation function

$$P[m,l] = \sum_{q=0}^{N-2} r^*[m,l+q]r[m,l+q+1], \quad (2)$$

whose samples can be iteratively calculated as $P[m,l+1] = P[m,l] - r^*[m,l]r[m,l+1] + r^*[m,l+N-1]r[m,l+N]$, where $m=0,\ldots,M-1$ and $l=0,\ldots,N-1$. Hence, considering the CP and pilot position in delay, $\theta_{\rm d}$ can be estimated by finding the peak of the timing metric $P_{\rm d}[m] = \sum_{l=0}^{N-1}P[m,l]$ as

$$\hat{\theta}_{\rm d} = \arg\max_m\{|P_{\rm d}[m]|\} - m_{\rm p} - L_{\rm CP}. \quad (3)$$

If $\theta < M$ is guaranteed, the TO estimate in (3) is accurate. However, when $\theta \geq M$ an additional TO estimation step in time dimension is also required.

B. TO estimation in time dimension

As a single estimation error in time leads to the large error of M samples, accurate estimation of $\theta_{\rm t}$ is of a paramount importance. The peak of the correlation function in (2) on the row $m'_{\rm p} = \hat{\theta}_{\rm d} + m_{\rm p} + L_{\rm CP}$ of the delay-time grid can provide an estimate of $\theta_{\rm t}$. However, as it will be shown in Section V, this estimate may not be accurate. This is because the time-selective channel may distort the pilot samples on the edges of the row $m'_{\rm p}$ on the delay-time grid and result in estimation error. Therefore, as a novel aspect of our proposed TO estimation technique, we exploit the multipath diversity of the channel to improve the estimation accuracy. In particular, multipath effect creates independent copies of the pilot signal at the delay bins $m = m'_{\rm p} + \ell$ for $\ell = 0,\ldots,L-1$, that can provide diversity gains in estimating $\theta_{\rm t}$. Hence, assuming that $\hat{\theta}_{\rm d}$ is accurate, $\theta_{\rm t}$ can be estimated by finding the peak of the timing metric $P_{\rm t}[l] = \sum_{m=m'_{\rm p}}^{m'_{\rm p}+L-1} P[m,l]^1$ as

$$\hat{\theta}_{\rm t} = \arg\max_l\{|P_{\rm t}[l]|\}. \quad (4)$$

To gain a deeper insight into the mechanism of exploiting multipath diversity in (4), we substitute the received pilot samples, $r_{\rm p}[m'_{\rm p}+\ell,l] = e^{\frac{j2\pi\varepsilon(Ml+m'_{\rm p}+\ell)}{MN}} h[\ell, Ml+m'_{\rm p}]X[m_{\rm p},l-\theta_{\rm t}] + \eta[m'_{\rm p}+\ell,l]$ for $\ell = 0,\ldots,L-1$, into the correlation function (2). Thus, at the exact timing estimate, $P[m'_{\rm p}+\ell,\theta_t] = \sum_{q=\theta_{\rm t}}^{N+\theta_{\rm t}-2} r^*_{\rm p}[m'_{\rm p}+\ell,q]r_{\rm p}[m'_{\rm p}+\ell,q+1]$ can be expanded as

$$P[m'_{\rm p}+\ell,\theta_t] = A_{\rm p}e^{j\phi_{\rm p}}\sum_{q=\theta_{\rm t}}^{N+\theta_{\rm t}-2}\left(\sum_{i=0}^{\Gamma-1}|\alpha_i|^2 e^{j\varphi^q_{i,i}}\delta[\ell-\ell_i] + \right.$$
$$\left. \sum_{i,i'=0,i\neq i'}^{\Gamma-1}\alpha^*_i\alpha_{i'}e^{j\varphi^q_{i,i'}}\delta_{\ell_i,\ell_{i'}} + \eta'[m'_{\rm p}+\ell,q]\right), \quad (5)$$

---

[1]If $m \geq M$ due to the pilot position $m_{\rm p}$, the delay and time indices in the timing metric will change to $(m \bmod M)$ and $(l + \lfloor\frac{m}{M}\rfloor)$, respectively.

where $\eta'[m'_{\rm p}+\ell,q] = \eta^*[m'_{\rm p}+\ell,q]\eta[m'_{\rm p}+\ell,q+1]$, $\varphi^q_{i,i'} = 2\pi\frac{\kappa_{\max}}{N}((\cos\psi_{i'} - \cos\psi_i)(q+\frac{m'_{\rm p}-\ell}{M}) + \cos\psi_{i'})$, $\delta_{\ell_i,\ell_{i'}} = \delta[\ell-\ell_i]\delta[\ell-\ell_{i'}]$, and $A_{\rm p} = \frac{|D[m_{\rm p},n_{\rm p}]|^2}{N}$ and $\phi_{\rm p} = \frac{2\pi(\varepsilon+n_{\rm p})}{N}$ represent the amplitude squared and the CFO affected phase of the pilot in delay-time, respectively. Since the noise samples and the path gains are independent and identically distributed random variables, taking expected value from (5), we have

$$\mathbb{E}\{P[m'_{\rm p}+\ell,\theta_t]\} = (N-1)A_{\rm p}e^{j\phi_{\rm p}}\rho[\ell]J_0(2\pi\frac{\kappa_{\max}}{N}), \quad (6)$$

where $\mathbb{E}\{\sum_{i=0}^{\Gamma-1}|\alpha_i|^2\delta[\ell-\ell_i]\} = \rho[\ell]$ is the total power that is received at delay tap ℓ, $\mathbb{E}_{i\neq i'}\{\alpha^*_i\alpha_{i'}\} = 0$, and $\mathbb{E}\{\eta'[m'_{\rm p}+\ell,q]\} = 0$. According to the Jakes' channel model [16], ψ is uniformly distributed in $[-\pi,\pi)$ and thus $\mathbb{E}\{e^{j2\pi\frac{\kappa_{\max}}{N}\cos\psi}\} = \frac{1}{2\pi}\int_{-\pi}^{\pi}e^{j2\pi\frac{\kappa_{\max}}{N}\cos\psi}d\psi = J_0(2\pi\frac{\kappa_{\max}}{N})$, where $J_0(.)$ denotes zeroth-order Bessel function of the first kind. Finally, from (6) and (4), one may realize that $\mathbb{E}\{|P_{\rm t}[\theta_t]|\} = (\frac{N-1}{N})|D[m_{\rm p},n_{\rm p}]|^2J_0(2\pi\frac{\kappa_{\max}}{N})|$ as $\sum_{\ell=0}^{L-1}\rho[\ell] = 1$. Hence, by combining the received pilot signals at the delay bins $m'_{\rm p}+\ell$ for $\ell = 0,\ldots,L-1$, using (4), we can collect the maximum received pilot energy and achieve multipath diversity gain. Additionally, from (3) and the above discussion, it is obvious that neither the CFO nor the pilot position in delay-Doppler plane have any effect on the TO estimates.

Fig. 3 depicts a snapshot of the timing metrics $P_{\rm d}[m]$ and $P_{\rm t}[l]$ at the SNR of 10 dB for an OTFS system with $M = 128$ and $N = 32$ delay and Doppler bins, respectively, for both LTI and LTV channels. After timing recovery of the received signal with the estimated TO, $\hat{\theta} = \hat{\theta}_{\rm d} + M\hat{\theta}_{\rm t}$, a residual timing error $\Delta\theta = \theta - \hat{\theta}$ may still remain in $\hat{r}[k] = r[k + \hat{\theta}_{\rm d} + M\hat{\theta}_{\rm t}]$. In Section V, we numerically evaluate the performance of our proposed TO estimation technique and show that the mean and variance of $\Delta\theta$ are very small that can be easily absorbed into the CP. The next step after timing acquisition is frequency synchronization. Thus, in the following Section, we develop a CFO estimation technique for OTFS.

IV. PROPOSED CFO ESTIMATION TECHNIQUE

As it was mentioned earlier, the phase difference between the pilot samples in the delay-time domain is $2\pi n_{\rm p}/N$. When the channel is LTI over each OTFS block, the delay-time pilot samples are affected by the same channel. Thus, the angle of $P[m_{\rm p},l]/e^{\frac{j2\pi n_{\rm p}}{N}}$ at the best timing instant $l = \hat{\theta}_{\rm t}$ in the absence of the noise is equal to $\hat{\phi} = \frac{2\pi\hat{\varepsilon}}{N}$. This leads to a reliable CFO estimate. However, when the channel is LTV, the adjacent pilot samples are affected by different channel coefficients that result in an inaccurate CFO estimate. To tackle this issue, similar to our proposed TO estimation technique in Section III, we exploit the multipath diversity of the channel. Based on our simulation results in Section V, this brings over an order of magnitude higher estimation accuracy than the case where multipath diversity is not considered. Hence, we can find the mean of the angles of the phase-corrected correlation functions $P[m,\hat{\theta}_{\rm t}]/e^{\frac{j2\pi n_{\rm p}}{N}}$ at the delay bins $m = m'_{\rm p},\ldots,m'_{\rm p}+L-1$ and estimate the CFO as

$$\widehat{\varepsilon} = \frac{N}{2\pi L}\left(\sum_{m=m'_{\rm p}}^{m'_{\rm p}+L-1}\angle P[m,\hat{\theta}_{\rm t}]\right) - n_{\rm p}, \quad (7)$$
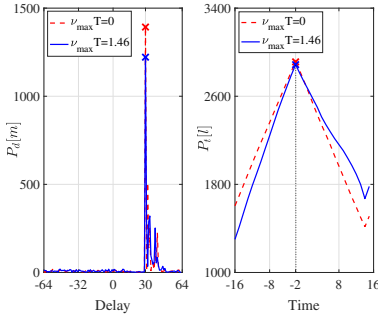
Fig. 3. A snapshot of the timing metrics $P_\mathrm{d}[m]$ and $P_\mathrm{t}[l]$ at SNR=10 dB for M=128 and N=32.
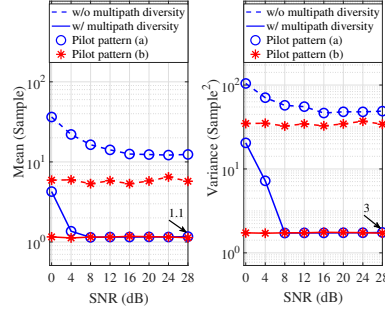
Fig. 4. Mean and variance of the proposed TO estimator for M=128 and N=32 and $\nu_\mathrm{max}T \approx 1.46$.
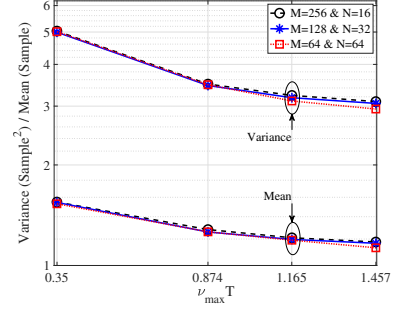
Fig. 5. Mean and variance of the proposed TO estimator at SNR=20 dB for pilot pattern (b).

where $\angle A$ represents the angle of the complex argument A. Therefore, the TO and CFO corrected signal can be obtained as $y[k] = e^{-\frac{j2\pi\hat{\varepsilon}k}{MN}} r[k + M\hat{\theta}_\mathrm{t} + \hat{\theta}_\mathrm{d}]$.

Based on the results of [7], in LTI channels, for a pilot with $\mathcal{I}$ identical parts, the CFO acquisition range is $[-\frac{\mathcal{I}}{2}, \frac{\mathcal{I}}{2})$. Consequently, as the pilot for OTFS has N identical samples, the acquisition range for our proposed technique is $[-\frac{N}{2}, \frac{N}{2})$ when the channel is LTI. However, Doppler spread in LTV channels imposes an ambiguity at the edges of the range. Hence, considering the Doppler effect, the acquisition range for reliable CFO estimation becomes $[-\frac{N-\kappa_\mathrm{max}}{2}, \frac{N-\kappa_\mathrm{max}}{2})$.

The estimated CFO in (7) can be considered as the normalized CFO that is contaminated by the phase variations of the LTV channel. Considering the guard symbols around the pilot, ignoring the noise and using the equations (1), (2), and (7), the CFO with estimation errors can be represented as

$$\widehat{\varepsilon} = \varepsilon + \frac{N}{2\pi L} \sum_{m=m'_\mathrm{p}}^{m'_\mathrm{p}+L-1} \angle C[m], \qquad (8)$$

where $C[m] = \sum_{q=0}^{N-2} h^*[m-m'_\mathrm{p}, Mq+m'_\mathrm{p}]h[m-m'_\mathrm{p}, M(q+1)+m'_\mathrm{p}]$. In Section V, we numerically evaluate the performance of our proposed CFO estimation technique. We show that both the CFO and TO estimation errors can be absorbed into the channel and compensated at the equalization stage. Even though in our developments, we only considered pilot pattern (a), in the following section, we show that our proposed synchronization techniques provide a satisfactory performance when any of the pilot patterns shown in Fig. 3 are deployed.

V. SIMULATION RESULTS

In this section, we numerically analyze the performance of our proposed TO and CFO estimation techniques. We consider an OTFS system with $M = 128$ and $N = 32$ delay and Doppler bins, respectively, unless otherwise is stated. One CP with the duration longer than the channel is appended at the beginning of each OTFS block. We use the extended vehicular A (EVA) channel model, [17], the bandwidth of 7.68 MHz and the delay-Doppler resolution $(\Delta\tau, \Delta\nu) = (130.21\,\mathrm{nsec}, 1.875\,\mathrm{kHz})$. When pilot pattern (a) is deployed, the power of the surrounding zero guard symbols are allocated to the pilot. This results in an increased pilot power by the factor of $(2L-1)N$ compared to the data symbols. As it is shown in [12], for pilot pattern (b), allocating the power of the guard symbols to the pilot does not lead to accurate channel

estimates. Thus, similar to [12], we set the pilot power 60 dB higher than data symbols and we choose $\hat{\kappa} = 2$. Throughout our simulations, the normalized TO and CFO values are randomly generated from a uniform distribution in the range $[-\frac{MN}{2}, \frac{MN}{2})$ and $[-\frac{N-\kappa_\mathrm{max}}{2}, \frac{N-\kappa_\mathrm{max}}{2})$, respectively.

In Fig. 4, we analyze the performance of our proposed TO estimation technique. We study the estimation error mean and variance as a function of signal to noise ratio (SNR), for the normalized Doppler spread of $\nu_\mathrm{max}T \approx 1.46$. The results in Fig. 4 show that our proposed technique leads to very small estimation error at SNRs above 8 dB for both pilot patterns. This estimation error originates from the fact that the correlation function in (6) at the correct timing depends on the PDP, $\rho[\ell]$. Hence, the delay tap ℓ from which the maximum power is received determines $\hat{\theta}_\mathrm{d}$ which is not necessarily the first tap. This error can be absorbed into the CP given that $L_\mathrm{CP} \geq L-1+\Delta\theta$ which will appear as a phase factor in the channel estimate. The higher estimation accuracy at low SNRs when pilot (b) is deployed is due to its higher power than pilot (a). Fig. 5 shows the behaviour of our proposed TO estimator as the normalized Doppler spread increases for different values of M and N and a fixed OTFS block length. An interesting observation here is the improved estimation accuracy as the Doppler spread of the channel increases. This is due to the diversity that is provided by the time-selective channel.

To solely analyze the performance of our proposed CFO estimator, we assume perfect knowledge of TO for the results provided in Figs. 6 and 7. In Fig. 6, we evaluate the MSE performance of our proposed CFO estimation technique as a function of SNR for two different values of Doppler spread and the two pilot patterns. As discussed in Section IV, CFO estimation accuracy can be substantially improved by exploiting the multipath diversity. Hence, in Fig 6, we observe that the accuracy of the CFO estimates can be improved by over an order of magnitude by exploiting the multipath diversity compared with the single-path case. The error floor that is observed in Fig. 6 is due to the Doppler spread of the LTV channel. As it is shown in Fig. 8, this error can be estimated as a part of the channel and compensated at the equalization stage. Similar to the TO estimation case, the superior performance of the pilot pattern (b) to pilot pattern (a) in SNRs below 20 dB is due to its higher power. In Fig. 7, we study the performance of our proposed CFO estimator as a function of Doppler spread for different pairs of M
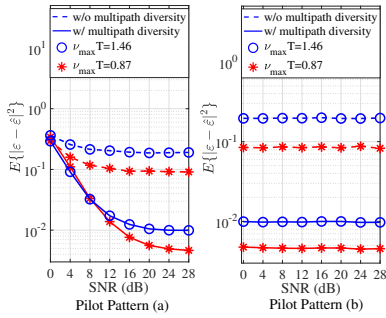
Fig. 6. MSE performance of the proposed CFO estimation technique for M=128 and N=32.
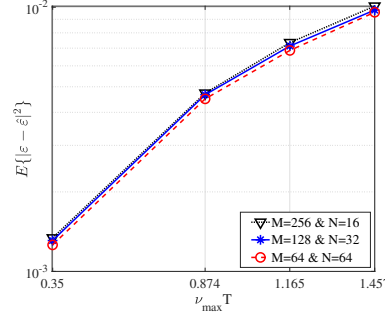

Fig. 7. MSE vs. Doppler spread of the proposed CFO estimator at SNR=20 dB for pilot pattern (b).
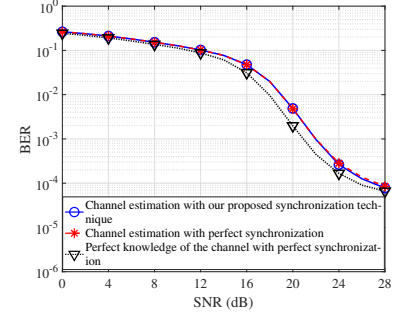

Fig. 8. BER of the proposed technique for M= 128, N=32 and $\nu_{\max}T$≈1.46.

and N, and a fixed OTFS block length. Our results show that the MSE performance degrades as the Doppler spread increases. To tackle this issue, one may choose to reduce M and thus alleviate the time-varying effects on the pilot samples. However, while reducing M leads to lower values of $\angle C[m]$ in equation (8), it results in a larger value of N that amplifies the MSE. Hence, we observe about the same performance for different pairs of M and N in Fig. 7.

Finally, in Fig. 8, we assess the overall BER performance of our proposed TO and CFO estimation techniques. We deploy the channel estimation method in [12] using the pilot pattern (b) that is more bandwidth efficient than pilot pattern (a). For channel equalization, we utilize the least squares minimum residual based technique with interference cancellation (LSMR-IC) in [18]. We set the case where the channel is estimated and we have perfect synchronization as a benchmark. As shown in Fig. 8, the BER performance of our proposed synchronization technique perfectly matches that of the benchmark. This proves the efficacy of our proposed technique. Fig. 8 shows that the small gap between the BER performance of our proposed technique, and a fully synchronous system with the perfect knowledge of the channel originates from the channel estimation error.

VI. Conclusion

In this letter, we proposed TO and CFO estimation techniques for OTFS. We showed that the periodic properties of the pilot signal that is used for channel estimation can be used for synchronization. Our proposed TO estimator forms a 2D correlation function and finds the start of each OTFS block by searching for a periodic sequence in delay and time dimensions. While a small TO estimation error in delay can be tolerated by using a slightly longer CP, a single estimation error in time leads to total misalignment of the received OTFS block. We addressed this issue and improved the TO estimation accuracy by exploiting the multipath diversity of the channel. We estimated the CFO by finding the angle of the aforementioned 2D correlation function at the best timing instant while considering the channel multipath diversity. Finally, we analyzed our proposed estimators in terms of the mean and variance of the TO estimation error and the MSE of the CFO estimates through simulations. We assessed the BER performance of our synchronization techniques and showed that our proposed estimators can provide the same BER performance as that of a fully synchronous system.

References

[1] R. Hadani, S. Rakib, M. Tsatsanis, A. Monk, A. J. Goldsmith, A. F. Molisch, and R. Calderbank, "Orthogonal time frequency space modulation," in *IEEE Wireless Commun. and Netw. Conf.*, 2017, pp. 1–6.

[2] F. Liu, C. Masouros, A. P. Petropulu, H. Griffiths, and L. Hanzo, "Joint radar and communication design: Applications, state-of-the-art, and the road ahead," *IEEE Trans. on Commun.*, vol. 68, no. 6, pp. 3834–3862, 2020.

[3] A. Aminjavaheri, A. Farhang, A. RezazadehReyhani, and B. Farhang-Boroujeny, "Impact of timing and frequency offsets on multicarrier waveform candidates for 5G," in *IEEE Signal Processing and Signal Processing Education Workshop*, 2015, pp. 178–183.

[4] M. D. Kapoor, S. and Y.-F. Huang, "Pilot assisted synchronization for wireless OFDM systems over fast time varying fading channels," in *IEEE Veh. Technol. Conf. Pathway to Global Wireless Revolution*, vol. 3, 1998, pp. 2077–2080.

[5] T. Schmidl and D. Cox, "Robust frequency and timing synchronization for OFDM," *IEEE Trans. on Commun.*, vol. 45, no. 12, pp. 1613–1621, 1997.

[6] H. Minn, V. Bhargava, and K. Letaief, "A robust timing and frequency synchronization for OFDM systems," *IEEE Trans. on Wireless Commun.*, vol. 2, no. 4, pp. 822–839, 2003.

[7] M. Morelli and U. Mengali, "An improved frequency offset estimator for OFDM applications," in *IEEE Communications Theory Mini-Conference*, 1999, pp. 106–109.

[8] M. Morelli, C.-C. J. Kuo, and M.-O. Pun, "Synchronization techniques for orthogonal frequency division multiple access (OFDMA): A tutorial review," *Proceedings of the IEEE*, vol. 95, no. 7, pp. 1394–1427, 2007.

[9] A. K. Sinha, S. K. Mohammed, P. Raviteja, Y. Hong, and E. Viterbo, "OTFS based random access preamble transmission for high mobility scenarios," *IEEE Trans. on Veh. Technol.*, vol. 69, no. 12, pp. 15 078–15 094, 2020.

[10] M. S. Khan, Y. J. Kim, Q. Sultan, J. Joung, and Y. S. Cho, "Downlink synchronization for OTFS-based cellular systems in high Doppler environments," *IEEE Access*, vol. 9, pp. 73 575–73 589, 2021.

[11] S. S. Das, V. Rangamgari, S. Tiwari, and S. C. Mondal, "Time domain channel estimation and equalization of CP-OTFS under multiple fractional Dopplers and residual synchronization errors," *IEEE Access*, vol. 9, pp. 10 561–10 576, 2021.

[12] P. Raviteja, K. T. Phan, Y. Hong, and E. Viterbo, "Embedded delay-Doppler channel estimation for orthogonal time frequency space modulation," in *IEEE Veh. Technol. Conf.*, 2018, pp. 1–5.

[13] P. Raviteja, Y. Hong, E. Viterbo, and E. Biglieri, "Practical pulse-shaping waveforms for reduced-cyclic-prefix OTFS," *IEEE Trans. on Veh. Technol.*, vol. 68, no. 1, pp. 957–961, 2019.

[14] A. Farhang, A. RezazadehReyhani, L. E. Doyle, and B. Farhang-Boroujeny, "Low complexity modem structure for OFDM-based orthogonal time frequency space modulation," *IEEE Wireless Commun. Lett.*, vol. 7, no. 3, pp. 344–347, 2018.

[15] F. Lampel, A. Alvarado, and F. Willems, "Orthogonal time frequency space modulation: A discrete Zak transform approach," *ArXiv*, vol. abs/2106.12828, 2021.

[16] W. Jakes, *Microwave Mobile Communications*. New York, Wiley, 1974.

[17] 3GPP, "Evolved universal terrestrial radio access (E-UTRA); base station (BS) radio transmission and reception," 3rd Generation Partnership Project (3GPP), TS 36.104 V15.3.0, 2018.

[18] H. Qu, G. Liu, L. Zhang, S. Wen, and M. A. Imran, "Low-complexity symbol detection and interference cancellation for OTFS system," *IEEE Trans. on Commun.*, vol. 69, no. 3, pp. 1524–1537, 2021.